

Hierarchical Frequency Control Scheme for Islanded Multi-Microgrids Operation

Nuno José Gil, and J. A. Peças Lopes, *Senior Member, IEEE*

Abstract—This paper presents a new hierarchical approach to deal with the problem of controlling frequency and active power generation of a medium voltage network comprising several microgrids and distributed generation sources operated in islanded mode.

The hierarchical approach described here should be cost effective and capable of dealing with large numbers of distributed microsources and performing tasks related to coordinated frequency control.

Index Terms—Distributed generation, microgrid, frequency control, hierarchical control.

I. INTRODUCTION

THIS paper presents a new hierarchical approach to deal with the problem of controlling frequency and active power generation of a Medium Voltage (MV) network comprising several microgrids and Distributed Generation (DG) sources operated in islanded mode.

A microgrid consists of a Low Voltage (LV) feeder with several microsources, storage devices and controllable loads connected on that same feeder (Fig. 1), including a local communication system and a hierarchical control structure managed locally by a MicroGrid Central Controller (MGCC).

The new concept of multi-microgrids is related to a higher level structure, formed at the Medium Voltage (MV) level, consisting of several LV microgrids and DG units connected on adjacent MV feeders. The possibility of having a large number of controllable microgrids, DG units and MV loads under Demand Side Management (DSM) control requires the use of a hierarchical control scheme that enables an efficient control and management of this kind of system. These concepts are being developed under the EU financed More-Microgrids Project.

In this paper it will be demonstrated how an intermediate managing control structure – the Central Autonomous Management Controller (CAMC) – can be used to accomplish some management tasks in this kind of multi-microgrid sys-

Nuno José Gil is with the Power Systems unit of INESC Porto, Porto and with the School of Technology and Management – Polytechnic Institute of Leiria (ESTG – IPLEiria), Leiria, Portugal (e-mail: ngil@estg.ipleiria.pt).

J. A. Peças Lopes is with the Power Systems unit of INESC Porto and with the Department of Electrical and Computer Engineering, Porto University, Porto, Portugal (e-mail: jpl@fe.up.pt).

tem, namely frequency control in case of MV network islanding and also load-following in islanded operation. The CAMC would relate to the Distribution Management System (DMS), under the responsibility of the Distribution System Operator (DSO). In fact, the CAMC may be seen as one DMS application which is in charge of one part of the distribution network that depends from one HV/MV substation (Fig. 2).

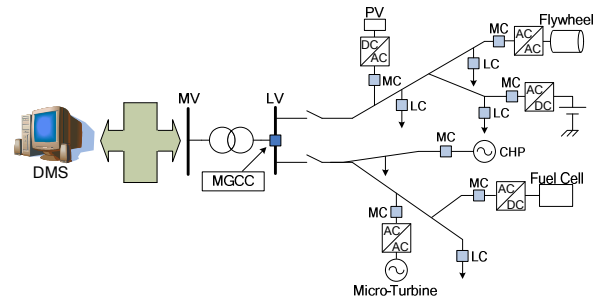


Fig. 1. Microgrid concept. The MV network would include several of these LV microgrids.

In order to test this concept, a dynamic simulation platform was developed exploiting *Eurostag v4.2* and *MATLAB* software packages.

This kind of change in the control paradigm for MV networks will require substantial modifications to the standard practice for distribution networks management. Currently, DG is typically disconnected during faults and MV islanded operation is not usually allowed, which could make this new control approach unfeasible. Therefore, protection and automation systems need to be adjusted or developed to allow MV islanded operation and, with that, all the related potential benefits.

II. HIERARCHICAL CONTROL

A. Introduction

The suggested hierarchical control system can be represented by the block diagram in Fig. 2. It will be shown how to possibly implement the Level 2 and Level 3 control autonomously, without any intervention from the DMS.

The CAMC will be the entity from where the commands for production change will be originated. The CAMC does not need to know the specific microgrid constitution as each of the microgrids is controlled and somewhat “hidden” by the corre-

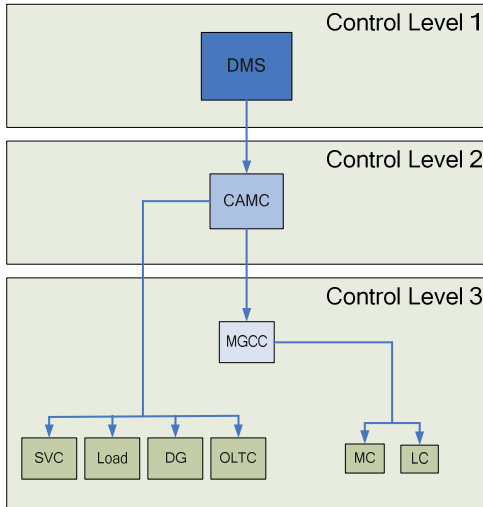


Fig. 2. Hierarchical control scheme. The implementation considered here only focuses on control levels 2 and 3.

sponding MGCC. However, the CAMC will still be able to perform control actions directly over other DG units, usually of bigger size than the ones under MGCC control.

The CAMC will react to power system frequency changes, in a way similar to the one implemented in regular Automatic Generation Control (AGC) functionalities [1]. The power generation change requested to the production system in case of frequency variation will be derived from the system frequency through a PI controller. Then, an economical allocation algorithm will distribute this power change among all the power generation units and MGCCs under CAMC control but only if they are willing, at that point in time, to participate in frequency regulation.

Each of the MGCCs will also allocate the generation request among its subordinate micro-generation units. Some of these do not usually have regulation capabilities (e.g., PV or wind generation, due to limitations in primary resource availability) and will not, in principle, be asked to change power generation.

This kind of decentralized control requires regular exchange of information among all intervening elements. As it is expected that this kind of information exchange will be subject to some delays that may not be negligible, such delays were included in the simulation.

The reason behind the choice of using power setpoint variations and not absolute power setpoints is related to the assumption that there could be a higher order control system, either automatic or manual, that would independently adjust micro-source or DG output to setpoints other than the system optimal ones. At one end of the spectrum, this “control system” could eventually be the microsource individual owners who would adjust microsources, for instance, according to their heating needs. Therefore, it is assumed that the CAMC would only act if strictly needed and would not try to globally change setpoints in order to achieve a near optimum point of operation of the system.

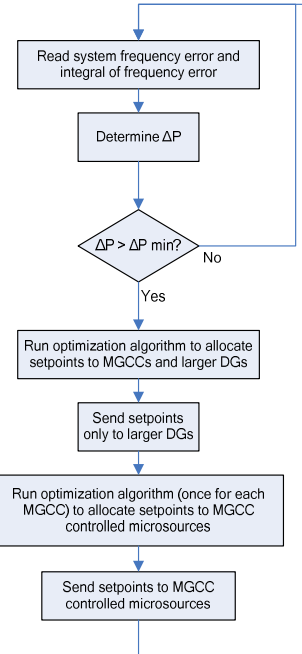


Fig. 3. Implementation flowchart. This procedure runs once each period T_s .

B. Control Details

The CAMC continuously samples the system frequency in order to identify if control actions are needed. However, it is not feasible to send control setpoints in real time to every MGCC and other DG. Because of this constraint, due mainly to communication systems limitations, the CAMC will react to system frequency changes every time interval T_s (sample time).

Therefore, each time T_s , the frequency error and the frequency error integral will be used to determine the additional power (1) to be requested to the available distributed generation under CAMC control. It should be noted that this additional power can have negative values if the frequency rises over its rated value. This way, the CAMC can respond to other disturbances, such as load loss while in islanded mode, commanding the distributed generation to reduce power output.

$$\Delta P = \left(K_p + K_i \frac{1}{s} \right) \times (f_{rated} - f) \quad (1)$$

If this required power variation is smaller than a specified threshold (i.e. the frequency is sufficiently close to its rated value) no action will be taken, as it is considered unnecessary.

On the other hand, if this required power variation is large enough, it will be necessary to determine how to distribute the power requests through the available sources. The unitary generation costs for each of the sources (MGCCs and other DGs) are used for this purpose.

The optimization is based on standard linear optimization techniques (2). In order to avoid globally changing setpoints

(e.g., decreasing production from expensive microsources and replacing them with less expensive ones), it was necessary to adjust the lower and upper bounds in (2) according to the ΔP value. If ΔP is positive, all the lower bounds are set to zero. Conversely, if ΔP is negative, all the upper bounds are set to zero. This assures that no microsource will decrease its production so that another can increase it (i.e., there will not be any automatic power transfers between microsources).

$$\begin{aligned} \min_x z &= c^T x \\ \text{subject to} & \sum x = \Delta P \\ & A_h x = b_h \\ & x \geq b_l \\ & x \leq b_2 \end{aligned} \quad (2)$$

Where:

- c is a vector of generation prices;
- x is a vector of generation setpoints;
- b_l are the smallest variations allowed;
- b_2 are the largest variations allowed;
- A_h and b_h define which generators participate in frequency regulation (b_h is all zeros and A_h is a zero matrix with ones in the diagonal in the i^{th} elements corresponding to units that cannot be adjusted).

This optimization is performed each period T_s and will originate a vector representing the power generation changes to be requested to the microgrids (MGCCs) and other DG units (e.g., CHP).

Now, each MGCC will have to request the microsources under its control to adjust their power generation levels. To this effect, an optimization procedure just like the one used for the CAMC will now be followed for each of the MGCCs, this time using the unitary generation cost for every microsource under control of each of the MGCCs.

The calculated differences in power generation will be used to determine the power setpoints to be sent to each microsource. Therefore, the power levels of the microsources at the end of the previous iteration would have to be known (Fig. 3). In order to do that, there are two choices: a) use the previous setpoint or b) use the previous power output. In steady-state these two values are quite similar. However, in transient conditions, these values can be rather different due to the large response times of some of the technologies usually available in microsources (e.g., fuel cells). It was found that using the previous setpoint values the system response was optimized due to the fact that less time would be wasted trying to increase the power output of sources with power setpoints already at their maximum values.

III. POWER SYSTEM MODELING

Eurostag was chosen as the main power system modeling platform. Some of the dynamic models of the power system

components came directly from *Eurostag*'s library but most of them, because of their non-standard nature, had to be implemented in this platform. This was the case of the Double Fed Induction Machine Wind Generator (DFIM), the Voltage Source Inverter (VSI), the GAST Microturbine and the SOFC Fuel Cell (the two last generators are used inside each microgrid).

The DFIM model is based on the approach described in [3]-[5] but includes additional modules for pitch and de-load control which could enable it to participate in frequency regulation.

The fuel cell and microturbine models are based on [6] and [7] with a few small adaptations.

The diesel generator is a small one, required only to enable the network to have some frequency regulation capability even when the hierarchical control is disabled.

The VSI model is quite simple and assumes that the inverter has some sort of storage element coupled to it. It is modeled as a power injector (as most of the user models in *Eurostag*) and is programmed to emulate the behavior of a synchronous machine, for example, injecting active power when system frequency drops. As the storage element is limited in capacity, the VSI can only inject power for a certain period of time before its reserves are depleted. This frequency response is proportional to grid frequency deviations, thus similar to the proportional control present in typical synchronous generators.

Although the presence of secondary control (PI controllers for frequency control) in the microsources is not necessarily incompatible with this hierarchical control scheme, it can happen that the economical allocation algorithm and the local microsource control may contradict each other. Therefore, all the microsource models used here have no intrinsic ability to participate in frequency regulation.

Eurostag is, however, unable to provide enough flexibility to allow for the implementation of complex control algorithms. Because of this limitation, the hierarchical control algorithm was implemented in *MATLAB* which calls *Eurostag* for simulation runs which last for the time defined as the CAMC sample time.

At the end of each run, the frequency value and the integral of the frequency error are extracted from *Eurostag* data files and used to determine the new setpoint values. Additionally, the delay times are also calculated and the new setpoint/time pairs are inserted in *Eurostag* data files, ready for another dynamic simulation run.

IV. TEST NETWORK STRUCTURE

The adopted test network represents what could possibly be the typical structure of a MV grid containing multiple microgrids and several kinds of larger DG systems (Fig. 4).

In this network one has assumed two zones, one rural and one urban (the loop in Fig. 4, on the left), both connected to a HV/MV substation. We can find in this system a relatively large number of microgrids, all connected to MV buses, and

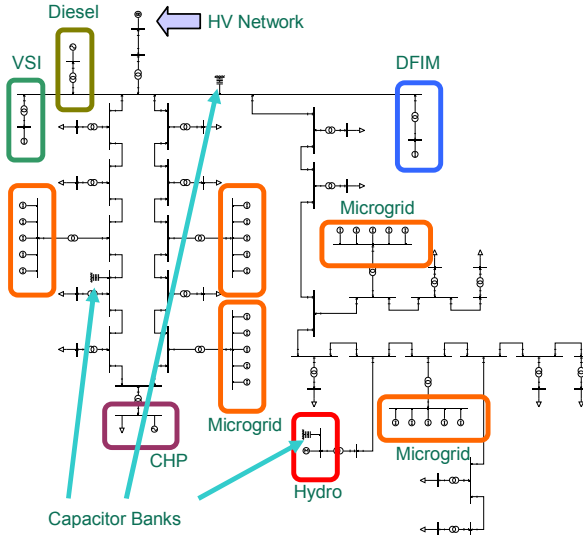


Fig. 4. Test network structure. The microgrid closest to the CHP unit is, with a 630 kVA transformer, a little larger than the others (400 kVA).

TABLE I
TEST NETWORK INITIAL ACTIVE POWER GENERATION

Source	Output Power (MW)	Rated Power (MW)
Diesel	0.7	1.2
VSI	0	1
DFIM	2	9
Hydro	1.5	2.8
CHP	1	2.1
Microgrids 1,2,3 & 5	0.1	0.25 (+0.15 VSI)
Microgrid 4	0.3	0.50 (+0.15 VSI)

also some other typically DG oriented generation systems: a small diesel group, a CHP unit, a doubly-fed induction machine (DFIM) corresponding to a wind-generator system and a storage element interfaced with the MV grid via a voltage source inverter (VSI). The active power generated by each of these units, in the considered scenario, can be found in Table I, along with the rated power of each of the units.

All the microgrids have the same mix of microsources: a small DFIM coupled to a wind-generator, a fuel cell, a micro-turbine, a photo-voltaic generator and a storage element connected to the grid via a VSI. In this particular case, four of the five microgrids are identical with the fifth one being larger than the others (Table I). All the microgrids are supposed to have a 150 kW / 50 kVAr load.

There are also some capacitor banks that are used for two purposes: they guarantee a better voltage profile throughout the network and, additionally, they provide sufficient reactive power to balance reactive generation and reactive load under islanded operation.

V. RESULTS OF A TEST CASE

The test case analyzed shows a situation where the MV network containing the microgrids is importing approximately

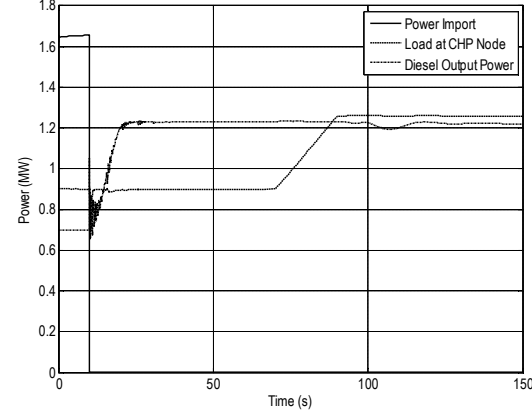


Fig. 5. Network disturbances (HV network disconnection and CHP node load change). Diesel generator response is also shown.

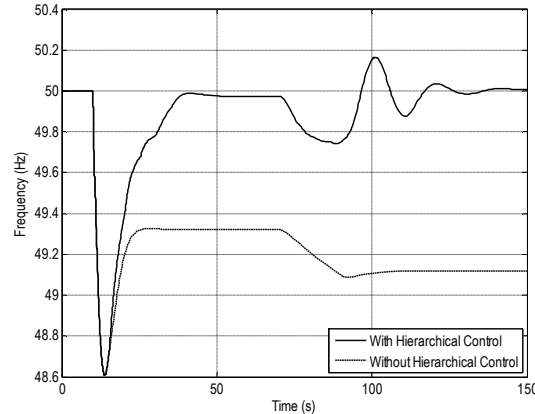


Fig. 6. Frequency deviation with and without hierarchical control.

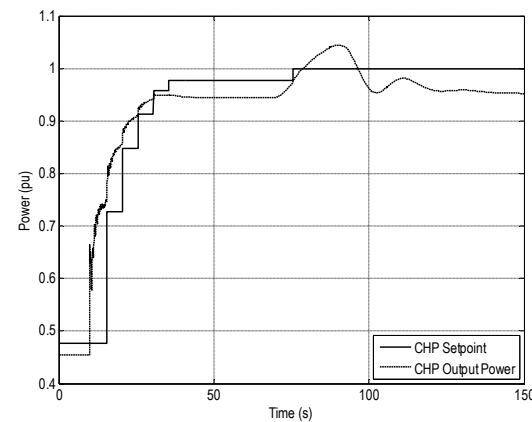


Fig. 7. DG setpoint sequence (of a CHP unit) as sent by the CAMC.

1.65 MW of active power from the upstream HV network, in order to be able to supply a total load of 7.55 MW.

Starting from this point, in steady-state, the HV/MV branch is disconnected at $t = 10$ s and the multi-microgrid system will become islanded (Fig. 5). At $t = 70$ s, the load at the node

TABLE II
PER UNIT ENERGY COSTS

Source	Type	Relative Cost
Fuel Cell	Microsource	20
Microturbine	Microsource	10
CHP	DG	7
Microgrids 1,2,3 & 5	MGCC	10
Microgrid 4	MGCC	8

These are relative costs. They don't represent any real world values and are meant only to help illustrate the operation of the optimization algorithm.

where the CHP unit is connected will begin to change at a rate of 2% per second for 20 s (Fig. 5).

The sample time in use is $T_s = 5$ s. Lower values can accelerate the system's response but could also create some stresses on the control system. The most adequate value will depend on the mix of microsources and other DGs on the system and could, eventually, be dynamically modified, depending on the currently available generation systems.

The relative costs per unit of energy adopted for this test case are shown in Table II. These costs are not real prices and are only meant to supply the optimization algorithm with different criteria for choosing some power sources over others.

The next results show how the several hierarchically controlled microgrids (and also some of the DG units) contribute to the system stability following an intentional islanding and also how they could help to improve load-following performance while in islanded operation.

The system's responses to this scenario can be seen in Fig. 6, which compares the frequency variations for the cases where the hierarchical control is enabled or disabled.

Right after disconnection from the HV grid, the frequency value decreases abruptly and then recovers, although without ever reaching the rated 50 Hz (Fig. 6). This is related to the fact that the diesel group, which is the only one to have a PI controller that actively tries to correct frequency errors, reaches its maximum power and cannot contribute any more (Fig. 5). Other generators that have somewhat marginal contributions to frequency control are the CHP unit and the VSIs, which have proportional controllers, incapable of correcting steady-state frequency errors.

The frequency evolution with hierarchical control (Fig. 6) demonstrates the potential of the method presented in this paper to help managing frequency. In fact, the setpoint modification commands sent to the microgrids enable the frequency to rise to the rated value. They also make it possible to have load variations without permanent changes in system operating frequency.

However, it should be noted that the hierarchical control scheme as shown here has little effect on the minimum frequency value following the studied disturbances. This is related not only to the response delays of some the controlled DG and microsources but also to the sample time used by the CAMC control loop. Additionally, some small delay also arises from the existence of a threshold on ΔP value. This threshold could be chosen to be large enough so that the sys-

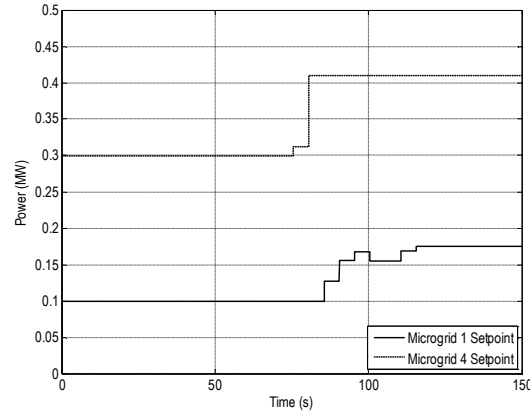


Fig. 8. Microgrid setpoints sent by the CAMC. Microgrid 4 is considered less expensive so its power setpoints increase first.

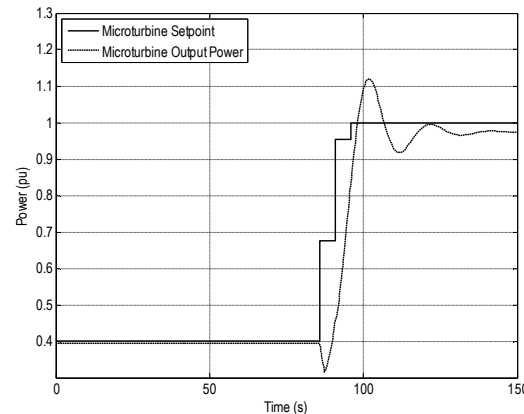


Fig. 9. Microturbine setpoint sequence.

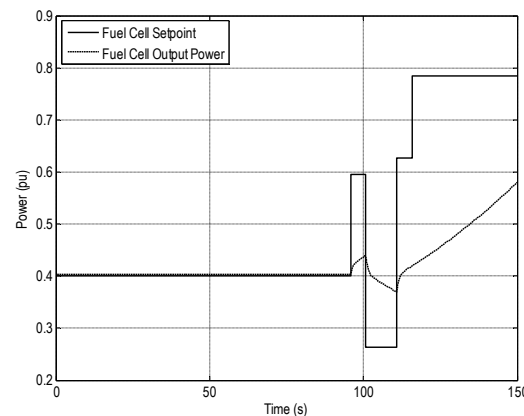


Fig. 10. Fuel cell setpoint sequence. Unit slow response is clearly visible.

tem is given a chance to recover the frequency by itself (e.g., through primary control, if applicable) before the hierarchical control system starts changing generation setpoints.

When the hierarchical control is activated, setpoints are being sent to the MGCCs. The CHP unit is also being controlled

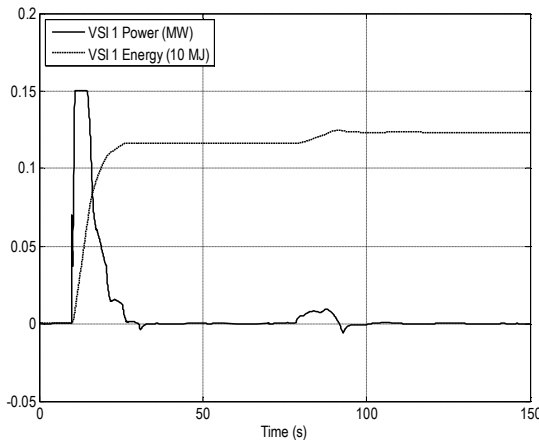


Fig. 11. VSI of microgrid 1 power output and total energy output.

to show how the hierarchical control can act on single power sources as well as on MGCCs.

The CHP unit is the first to be requested to respond (Fig. 7), because it's also the less expensive one. It is then followed by microgrid 4 (Fig. 8) and only after this microgrid reaches its maximum power output requests are made to the other microgrids (microgrid 1 is the only one shown in Fig. 8, but others are the same).

The effect of the communication delay can be observed, for the microgrid 1 setpoint curve, near the 100 s vertical grid line (the descending step takes place 0.5 s after $t = 100$ s). Due to the magnitude of the rest of the time constants involved in this simulation, these delays could eventually be ignored.

The next pictures show examples of the setpoint values and output power (the latter in a dashed line) for the microturbine (Fig. 9) and fuel cell (Fig. 10) in one of the microgrids. These setpoints are assigned by the corresponding MGCCs and are being sent only to fuel cells and microturbines as the remaining microsources are not usually controllable.

Again, the unitary energy cost of the microsources plays an important role in the time evolution shown. The microturbine is much less expensive to operate than the fuel cell, therefore it is the first one to increase its setpoint and, conversely, the fuel cell is the first microsource to decrease its power production (when the frequency drops below rated values for some time).

As the VSIs have a limited capacity storage element, the situation at the end of the simulation in Fig. 6 cannot last indefinitely. After the storage capacity is depleted, the VSIs will stop contributing and the frequency value will suffer another drop. In Fig. 11 it is possible to see how the VSIs try to respond to frequency drops. There's also an indication of the accumulated energy output. If it rises above a specified value (2 MJ, in this case) the energy storage is considered depleted and no power is injected in the network.

VI. CONCLUSIONS

The approach described here to implement a hierarchical control system capable of dealing with large numbers of distributed microsources has shown to be able to cope with tasks related to coordinated frequency control.

The setpoint modification commands sent to DG units and microgrids enable the frequency to return to the rated value after disturbances such as islanding and load variations.

The hierarchical control system should also be easier to implement because the DMS and the CAMC do not need to have direct access to the data relative to the (possibly innumerable) microsources in every microgrid connected to the MV network.

Hierarchical control provides, therefore, a flexible and cost effective way to efficiently control networks with multiple microgrids and high penetration levels of DG.

VII. REFERENCES

- [1] P. Kundur, *Power System Stability and Control*, New York: McGraw-Hill, 1994.
- [2] G. S. Stavrakakis and G. N. Kariniotakis, "A General Simulation Algorithm for the Accurate Assessment of Isolated Diesel - Wind Turbines Systems Interaction. Part I: A General Multimachine Power System Model," *IEEE Transactions on Energy Conversion*, vol. 10, pp. 577-583, 1995.
- [3] N. Jenkins, L. Holdsworth, and X. Wu, "Dynamic and Stead-State Modelling of the Doubly-Fed Induction Machine (DFIM) for Wind Turbine Applications," MCEE UMIST 14th January 2002.
- [4] A. Vladislav, "Analysis of Dynamic Behaviour of Electric Power Systems with Large Amount of Wind Power," Tese de Doutoramento, Technical University of Denmark, 2003.
- [5] J. G. Slootweg, H. Polinder, and W. L. Kling, "Dynamic Modelling of a Wind Turbine with Doubly Fed Induction Generator," presented at IEEE PES Summer Meeting, Vancouver, 2001.
- [6] Y. Zhu and K. Tomsovic, "Development of models for analyzing the load-following performance of microturbines and fuel cells," *Electric Power Systems Research*, 2002.
- [7] M. Nagpal, A. Moshref, G. K. Morison, and P. Kundur, "Experience with Testing and Modeling of Gas Turbines," 2000.